International Journal of Heat and Mass Transfer 58 (2013) 735–739

Contents lists available at SciVerse ScienceDirect

International Journal of Heat and Mass Transfer

journal homepage: www.elsevier.com/locate/ijhmt

Liquid–solid mass and heat transfer behavior of a concentric tube airlift reactor

M.H. Abdel-Aziz [a,b,*], I. Nirdosh [a], G.H. Sedahmed [b]

[a] Chemical Engineering Department, Lakehead University, Thunder Bay, Ontario, Canada
[b] Chemical Engineering Department, Alexandria University, Alexandria, Egypt

ARTICLE INFO

Article history:
Received 17 June 2012
Received in revised form 10 November 2012
Accepted 14 November 2012

Keywords:
Mass transfer
Airlift reactor
Electrochemical reactor
Heterogeneous reactions
Heat transfer
Air pollution control

ABSTRACT

Rates of liquid–solid mass transfer and heat transfer (by analogy) at the downcomer of concentric tube airlift reactor were studied by an electrochemical technique which involved measuring the limiting current of the cathodic reduction of ferricyanide ion in a large excess of sodium hydroxide. Variables studied were: superficial air velocity, physical properties of the solution and the effect of surface active agents. The data were correlated by the equation:

$$j = 0.096(\mathrm{Re} \cdot \mathrm{Fr})^{-0.14}$$

Surface active agents were found to decrease the rate of mass transfer by an amount ranging from 54% to 84% depending on surfactant concentration. The importance of the present results for the design and operation of cooling jackets used to cool airlift reactors was highlighted. Also the possibility of using airlift reactors as low cost electrochemical and catalytic reactors to conduct liquid–solid diffusion controlled reactions, especially those involving gaseous reactants, was discussed, as in electrochemical air pollution control to remove pollutants such as SO_2, Cl_2, H_2S and nitrogen oxides, in which case the airlift reactor acts simultaneously as a gas scrubber and a reactor.

1. Introduction

In view of their simple design and operation (no moving parts), high rates of gas–liquid mass transfer and efficient mixing in the liquid phase and their low energy consumption compared to mechanically stirred reactors [1–3], airlift reactors have been used widely in biochemical processes, wastewater treatment, ore leaching in the Pachuca tank and in chemical technology to conduct gas–liquid reactions. Airlift reactors are modified bubble columns which are divided into two channels connected from top to bottom, a channel for upward gas sparging (the riser) and a channel for downward solution circulation (the downcomer). The difference in hydrostatic pressure arising from the difference in gas–liquid dispersion between the two regions induces liquid circulation in the contactor thus enhancing the macro scale mixing in the liquid phase compared to that of bubble columns. Apart from the processes which currently use airlift reactors there is considerable potential to extend the use of airlift reactors to other fields such as liquid–solid diffusion controlled catalytic and electrochemical processes. Although much work has been done on the hydrodynamic behavior and gas–liquid mass transfer behavior of airlift reactors, little has been done on their liquid–solid mass transfer behavior despite the potential importance of the subject. The aim of this study was to investigate the rate of liquid–solid mass transfer at the wall of a cylindrical downcomer concentric with a cylindrical riser with the objective of developing an airlift electrochemical reactor and an airlift catalytic reactor suitable for conducting liquid–solid diffusion controlled reactions such as removal of heavy metals from waste solution, electroorganic synthesis, electrochemical reactions involving gaseous reactants such as alkenes epoxidation (e.g., production of propylene oxide from propylene), electrochemical synthesis of H_2O_2 by cathodic reduction of oxygen in alkaline solution and electrochemical air pollution control to remove pollutants such as SO_2, H_2S, Cl_2 and nitrogen oxides [4]. The reactor can also be used for catalytic removal of organic pollutants [5], photocatalytic reactions [6], catalytic organic synthesis [7], and immobilized enzymes catalytic reactions [8]. By virtue of the analogy between heat and mass transfer the present study is useful for calculating the rate of heat transfer between cooling jackets and airlift reactors where exothermic reactions take place. Beside assisting in the calculation of the inner side heat transfer coefficient of the cooling jacket, the present study can be also used to predict the rate of corrosion of downcomer metallic wall. Corrosion of steel or copper is known to be diffusion controlled which depends on the rate of mass transfer of dissolved oxygen to the wall [9]. Although some work has been done on the mass transfer behavior of gas sparged electrochemical and catalytic reactors where diffusion controlled reactions takes place [10–13], no study was reported on the liquid–solid mass transfer behavior of airlift reactors except for

* Corresponding author at: Chemical Engineering Department, Alexandria University, Alexandria, Egypt. Tel.: +20 35745962.

E-mail address: helmy2002@gmail.com (M.H. Abdel-Aziz).

0017-9310/$ - see front matter © 2012 Elsevier Ltd. All rights reserved.
http://dx.doi.org/10.1016/j.ijheatmasstransfer.2012.11.054

Nomenclature

A	Cathode area
A_r, A_d	cross sectional area of the riser and downcomer, respectively
a	constant
C	ferricyanide concentration
C_p	fluid heat capacity
d_e	annulus equivalent diameter ($d_o - d_i$)
d_o	outer annulus diameter
d_i	inner annulus diameter
D	diffusivity of ferrocyanide
F	Faraday constant (96500 C mol^{-1})
g	acceleration due to gravity
h	heat transfer coefficient
I	limiting current
k	mass transfer coefficient
$\bar{k}$	thermal conductivity of the fluid
k_b	frictional loss coefficient in the bottom zone
L	gas–liquid dispersion height in the reactor
V	solution circulation velocity
V_g	superficial air velocity
Z	number of electrons involved in the reaction
Nu	Nusselt number $\left(\frac{hd_e}{\bar{k}}\right)$
Pr	Prandtl number $\left(\frac{\mu C_p}{\bar{k}}\right)$
Re	Reynolds number $\left(\frac{\rho V_g d_e}{\mu}\right)$
j	mass or heat transfer j factor $\left(\mathrm{St} \cdot \mathrm{Sc}^{0.66}\right)$
St	Stanton number $\left(\frac{k}{V_g}\right)$
Fr	Froude number $\left(\frac{V_g^2}{g d_e}\right)$
Sh	Sherwood number $\left(\frac{kd_e}{D}\right)$
Sc	Schmidt number $\left(\frac{\mu}{\rho}\right)$
ρ	solution density
$\in_r$, $\in_d$	gas holdup in the riser and the downcomer, respectively
μ	solution viscosity
ν	kinematic viscosity of the solution $\left(\frac{\mu}{\rho}\right)$

airlift slurry reactors [14]. Since the present reactor could be used for processing solutions containing surface active agents, for instance, removal of heavy metals from electroplating waste solution containing surfactants, electro-organic synthesis from solutions containing quaternary ammonium salts and removal of organic pollutants which are surface active by catalytic oxidation, it would be worthwhile to study the effect of surface active agents on the mass transfer behavior of airlift reactors. The mass transfer behavior of airlift reactor was studied under different conditions by measuring the limiting current of the cathodic reduction of $K_3Fe(CN)_6$ in a large excess of NaOH to eliminate transfer of ions by electrical migration in order to satisfy the analogy between heat and mass transfer [15,16]. In view of this analogy the present electrochemical technique has been used widely to measure rates of heat transfer under different hydrodynamic conditions [13,16]. A nickel plated copper cylinder cathode formed the downcomer of the reactor and a concentric stainless steel cylinder riser formed the anode of the reactor. This annular geometry offered the advantage of uniform current and potential distribution which is a highly desirable property especially for electro-organic synthesis where a high selectivity is obtained [17,18]. The use of annulus (the downcomer) as an electrochemical reactor has the advantage over gas-sparged electrochemical reactors that the gas hold up in the downcomer is much lower than that in the gas-sparged reactor [19]. Accordingly the specific resistance of the solution in the downcomer of the airlift reactor is less than that in gas-sparged reactor [20]. As a consequence the voltage drop, the cell voltage and the electrical energy consumption are less in the case of airlift reactors.

2. Experimental technique

The apparatus (Fig. 1) consisted of the cell and electrical circuit. The cell consisted of Plexiglass cylindrical container of 10 cm diameter and 25 cm height lined with cylindrical nickel sheet which formed the cell cathode. A vertical cylindrical stainless steel tube of 7 cm diameter and 15 cm height was positioned coaxially with the Plexiglass container, the distance between the lower end of the stainless steel tube and the flat bottom of the Plexiglass container was 2.2 cm. The stainless steel tube acted as a riser for the airlift reactor and an anode for the annular cell. The annulus between the stainless steel tube and the Plexiglass container wall formed the downcomer of the airlift reactor. The ratio of the cross-sectional areas of the riser (A_r) and the downcomer (A_d) was ≈1, and according to Gavrilescu and Tudose [21], this area ratio gives the highest liquid flow rate in the riser. The flat bottom of the Plexiglass container was made of a sintered glass (G-3) whose bores were blocked by a plastic washer glued to the sintered glass bottom except for the central 7 cm diameter area lying below the riser. A conical Plexiglass gas inlet was fitted to the bottom of the Plexiglass container. The electrical circuit consisted of 12 V d.c. power supply with a voltage regulator and a multirange ammeter connected in series with the cell. Before each run the cell

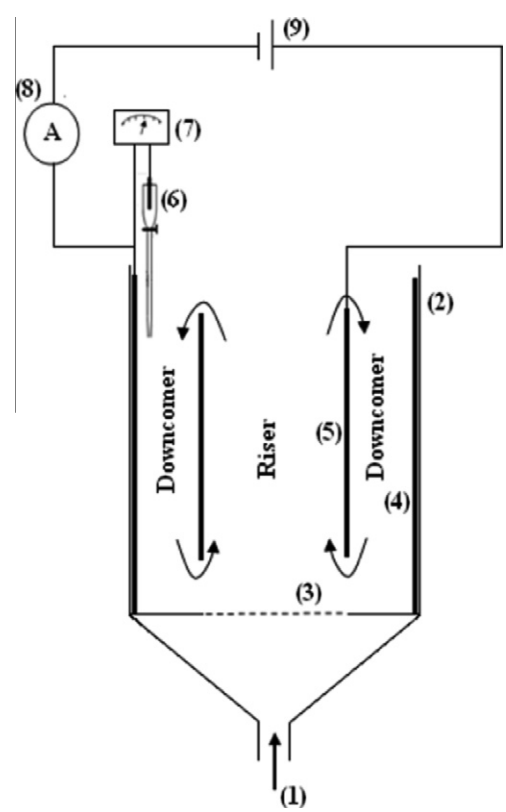

Fig. 1. Experimental apparatus. (1) Gas inlet, (2) Plexiglass container, (3) Porous bottom, (4) Nickel sheet cathode, (5) Stainless steel sheet anode, (6) Luggin tube, (7) Voltmeter, (8) Ammeter, and (9) D.C power supply.